American Journal of Engineering Research (AJER) **2019**
American Journal of Engineering Research (AJER)
e-ISSN: 2320-0847 p-ISSN : 2320-0936
Volume-8, Issue-7, pp-116-123
www.ajer.org
Research Paper Open Access

DSP Based Battery Charger Control System Using Embedded Code Generation for Thyristor Rectifier

Yasemin ÖNAL†, Metin KESLER*
†Corresponding Author **:**Dept. of Electrical and Electronic Engineering, Bilecik Seyh Edebali University, Bilecik, Turkey.
Corresponding Author ORCID ID: 0000-0003-0173-0948
*Dept. of Computer Engineering, Bilecik Seyh Edebali University, Bilecik, Turkey

ABSTRACT: A battery is a device usually used to store power and deliver it to the energy system when the power is not enough for the system. A battery charger consists of a three-phase thyristor, also known as silicon controlled rectifier (SCR), which is suitable for high power outputs such as induction heating and DC arc furnaces. In this paper, a new DSP based controller using Embedded Code Generation (ECG) for the battery charger is presented. This controller provides constant battery current and voltage control. The simulation of the proposed controller is created by using of computational PLL and C blocks in PSIM. The proposed controller is transmitted to SimCoder to obtain C-code. SimCoder generates the project outputs to the Code Composer Studio (CCS). In a battery charge controller design, when the users request to modify the codes for DSP and create a prototype, as well as creating C codes for CCS; the embedded code generation ECG provides a very fast solution. As a simulation circuit, different output powers are simulated following the proposed controller. The proposed controller is experimentally tested using a prototype. The experimental prototype includes voltage sensors, current sensors, the driver and chargers power module, DSP board. The proposed DSP based controller is quite simple, understandable and easy to implement.
KEYWORDS: AC-DC converters; Battery chargers; Embedded digital signal processor; Phase locked loop PLL; Embedded code generation

---

Date of Submission: 30-06-2019 Date of Acceptance: 19-07-2019

I. INTRODUCTION

All sorts of electronic devices use rechargeable batteries such as movable devices, UPS systems and electric vehicles. Therefore, battery chargers play a very important role in recharging batteries efficiently and extending the battery life [1-3]. In the literature, the conventional full-bridge converter, DC-DC boost converter, an AC-DC converter have been the most used topologies for battery chargers[4-9]. But, when the output of the DC-DC converter varies considerably, as in battery charging applications, conventional converters cannot be optimized for power conversion. Several battery chargers consisting of resonant topology or Cuk topology have been studied [10-11]. Usually, in order to supply ZVS in resonant converters, an excess quantity of circulating reactive current is required, particularly for a very extensive range of load variations, as is the case in battery charging practices. The hybrid-type DC-DC converters have been researched recently [12-13].

However, battery chargers require to change the battery voltage according to the stable battery current and then, chargers require to change the battery current according to the stable battery voltage. This process and high power output can be realized using three-phase SCR rectifier. Owing to the high power output and low cost of three-phase SCR topology based rectifiers, they are still widely used in industrial applications, such as electric arc furnaces, electro-chemical processes, and medium-voltage direct current transmissions [14-16].

Traditional battery chargers use analog controllers. These controllers can adjust the charge voltage and provide current control. But the compensation parameters are generated to resistor and capacitors in the analog controller. For digital control, the compensation parameters are implemented digitally and they can be mitigated. Different digital controllers for the battery chargers have been researched [17-18]. These controllers use a variety of battery voltages and temperatures to achieve a fast charging process. Lately, a very fast digital signal processor (DSP) has become a common category of study in the field of the digital controllers for the battery chargers in the literature [19-21]. A DSP provides a robust hardware sample circuit platform for real-time, closed loop control development with microcontrollers. The DSP is a great tool to change by requirement and verified solutions for many common power electronics practices, containing motor control, digital power supplies, PV inverters, and digital LED applications.

In this study, the new DSP based controller using embedded code generation (ECG) for the battery chargers with three-phase SCR rectifier to obtain high power output is proposed. The proposed controller of the battery chargers is developed by the use of computational blocks, phase locked loops (PLL) and C blocks in PSIM. As a simulation circuit, different output powers are simulated following the proposed controller. The experimental system includes voltage sensors, current sensors, the driver and chargers power module, DSP board.

II. MATERIALS AND METHODS

The battery current has to stay at the constant value while the battery voltage increases, and then, the battery current has to decrease while the battery voltage stays at the constant value in the battery chargers. The schematic circuit diagram of battery chargers that is three-phase rectifier consisting of SCR is designed as shown in Figure 1.

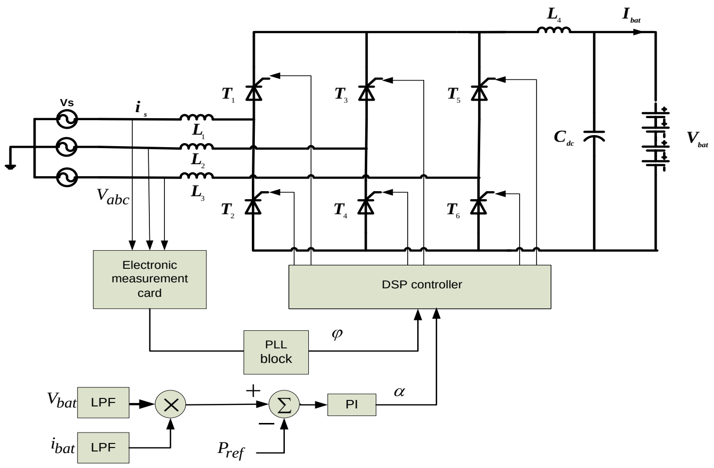

Figure 1 Complete schematic circuit diagram of battery chargers

The SCR rectifier, which consists of T_1, T_2 T_3, T_4, T_5, and T_6 switches, can be operated as a rectifier to supply the power for the battery charger. This topology consists of 6 SCR and 3 inductors on the AC input part to balance for disturbances in the source current and to obtain sinusoidal current signals.
The battery voltage is obtained from equation 1.

$$\begin{aligned} V_{bat} &= \frac{6}{2\pi}\int_{-\pi/6+\alpha}^{\pi/6+\alpha} V_{hm}\cos(\omega t)d(\omega t) = \frac{3}{\pi}V_{hm}\left|\sin(\omega t)\right|_{-\pi/6+\alpha}^{\pi/6+\alpha} \\ &= \frac{3}{\pi}V_{hm}\left[\sin\frac{\pi}{6}\cos\alpha + \cos\frac{\pi}{6}\sin\alpha + \sin\frac{\pi}{6}\cos\alpha - \cos\frac{\pi}{6}\sin\alpha\right] \\ &= \frac{3\sqrt{2}}{\pi}V_h\cos\alpha = \frac{3\sqrt{6}}{\pi}V_f\cos\alpha \end{aligned} \quad (1)$$

where α is the SCR firing angle and V_{hm} is the maximum value of AC voltage between phases. The battery voltage can be adjusted continuously by changing the α value. The α value has to be decreased to obtain the similar voltage.

The parameters of the system are shown in Table I. The battery voltage is determined according to the storage battery. Various power values are tried to verify the control system achievement.

Table I. System Parameters

Parameter	Symbol	Value
Output Power	P	2500W
Three phase line to line AC voltage	V_{ab}	190V
Line frequency	f	50Hz
Inductance	L	1.2mH
Battery voltage	V_{bat}	250V

Figure 2 shows the algorithm of proposed controller for battery chargers. The algorithm of proposed controller consists of LPF, DC energy computing, a PLL algorithm and synchronous reference frame equations. The measured battery voltage and current are processed through a LPF to eliminate the noise on the measurements. The battery voltage and current are used to DC energy computing. The calculated power is compared with reference power Pref. The SCR angle α is obtained from the PI controller output.

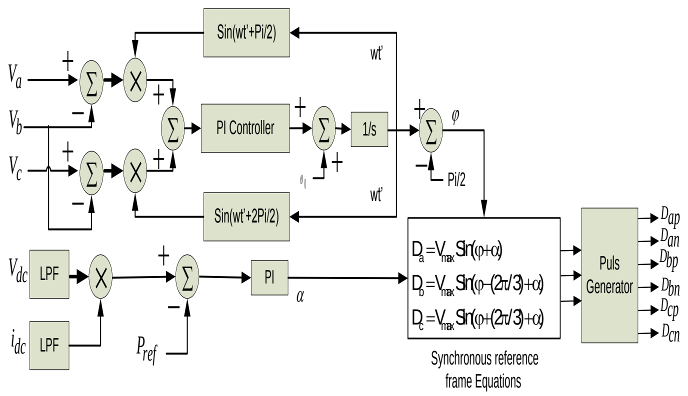

Figure 2 The algorithm of proposed controller for battery chargers

The three-phase line voltages V_a and V_b are measured and the grid voltage transformation angle φ is obtained from equation 2.

$$V_{ab} = V_a - V_b$$

$$V_{cb} = V_c - V_b \qquad (2)$$

The measured voltages V_{ab} and V_{cb} are multiplied by the feedback currents with unity amplitude to calculate three-phase instantaneous power P_{3a} by using equation 3.

$$P_{3a} = \sin(wt' + pi/2) \times V_{ab} + \sin(wt' + 2pi/2) \times V_{bc} \qquad (3)$$

The obtained instantaneous active power P_{3a} is passed to PI control block. The reference fundamental angular frequency 2πf is added to output of the PI control block for regulating the PI output. This block output is passed to $1/s$ and wt' is acquired. But the obtained wt' forwards $pi/2$ to the source fundamental frequency. For this reason, the $pi/2$ is reduced to the output of the $1/s$ block for obtaining source frequency and grid voltage transformation angle φ are achieved. The PI controller output α and the PLL output φ are used for calculating the synchronous reference frame equations D_a, D_b, D_c by using equation 4.

$$D_a = V_{\max} \sin(\varphi + \alpha)$$

$$D_b = V_{\max} \sin(\varphi - (2\pi/3) + \alpha) \qquad (4)$$

$$D_c = V_{\max} \sin(\varphi + (2\pi/3) + \alpha)$$

The pulse generator produces SCR switching signals for the battery chargers. The algorithm of the ECG is shown in Figure 3.

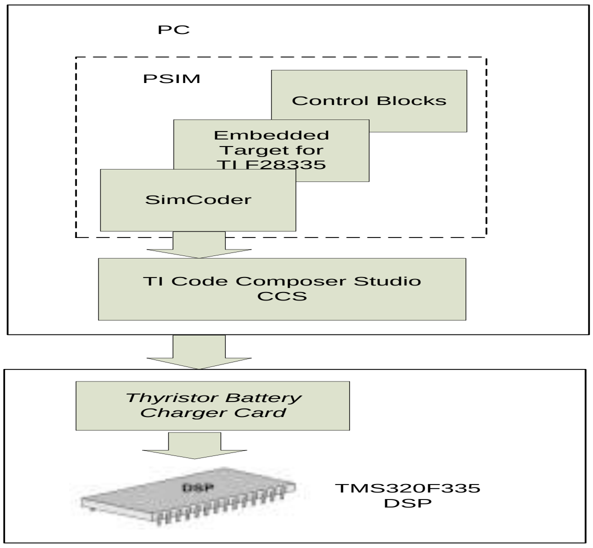

Figure 3 Operation of embedded code generation ECG

The proposed controller of the battery chargers is developed by the use of control blocks which consist of computational blocks, Embedded-Target block in PSIM. This control system is transmitted to SimCoder to obtain C-code. SimCoder also generates all project outputs to the TI-CCS. The TI-CCS loads the generated code to the DSP by using an emulator which exists on battery chargers. Therefore, in a battery charge controller design, when the users request to modify the codes for DSP and create a prototype, as well as creating C codes for CCS; the embedded code generation ECG provides a very fast solution.

III. RESULTS AND DISCUSSION

A simulation study is developed to show the process of three-phase SCR battery chargers. The simulation circuit of the proposed controller for the battery chargers using PSIM is shown in Figure 4. The simulation circuit consists of three-phase SCR rectifier, current, voltage sensors, electronic measurement circuit, alpha controller block. The battery voltage, battery current, three-phase line voltages V_a, V_b and V_c are measured by the current and voltage sensors, and they are sent to electronic measurement circuit. DC power is calculated and is compared with P_{ref} . The grid voltage transformation angle φ is obtained from the PLL block. The alpha controller block produces SCR switching signals for the battery charger. The C code of the proposed controller is obtained from PSIM. This procedure offers a rapid algorithm development and code generation.

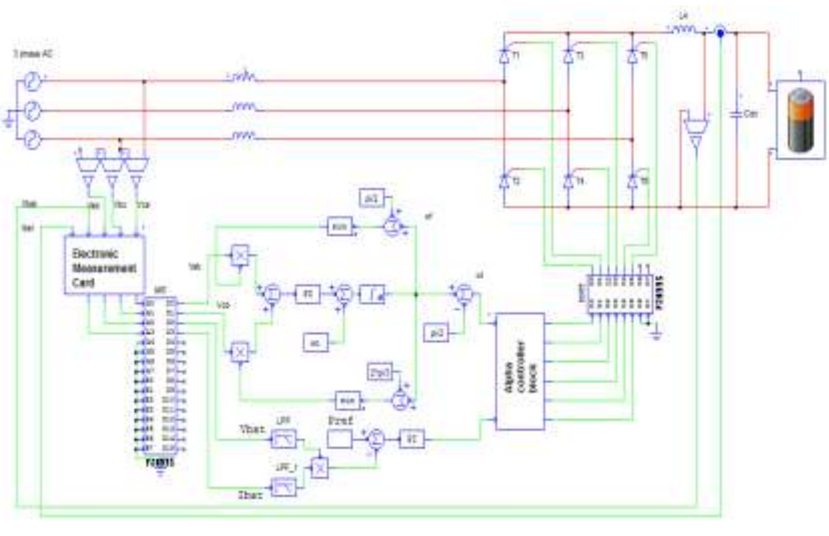

Figure 4 The simulation circuit of proposed controller for battery chargers.

Figure 5 shows the battery voltage, battery current, three-phase currents, active power and SCR firing angle. The battery currents are 25A, 40A and 15A respectively. Demanded power is 10kW between 0.1-0.2 seconds, 16kW between 0.2-0.35 seconds and 6kW between 0.35-0.5 seconds. The proposed controller performs the battery loading.

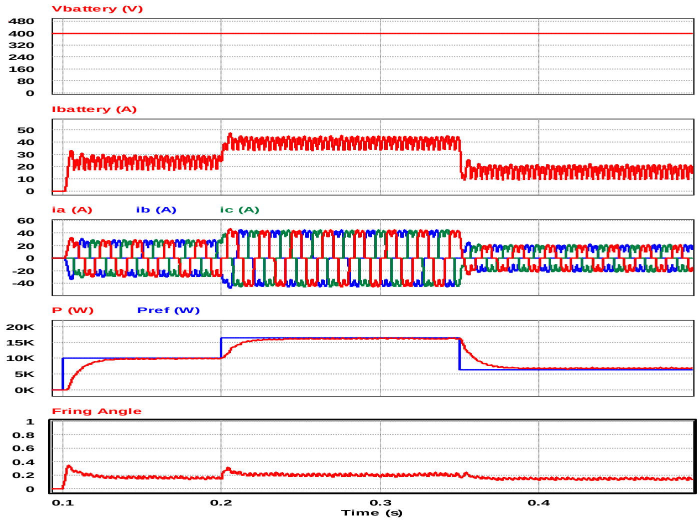

Figure 5 The battery voltage, battery current, three phase currents, active power and SCR firing angle obtained from proposed controller

Figure 6 shows the zoomed battery voltage, battery current, three phase currents, active power and SCR firing angle. The controller achievement is presented in the zoomed version of the transition after the command power changes from 10kW to 16kW in Figure 6a and changes from 16kW to 6kW in Figure 6b. The controller responds to the power commands expeditiously. The proposed controller is implemented for a sample circuit, and the circuit validity is tried.

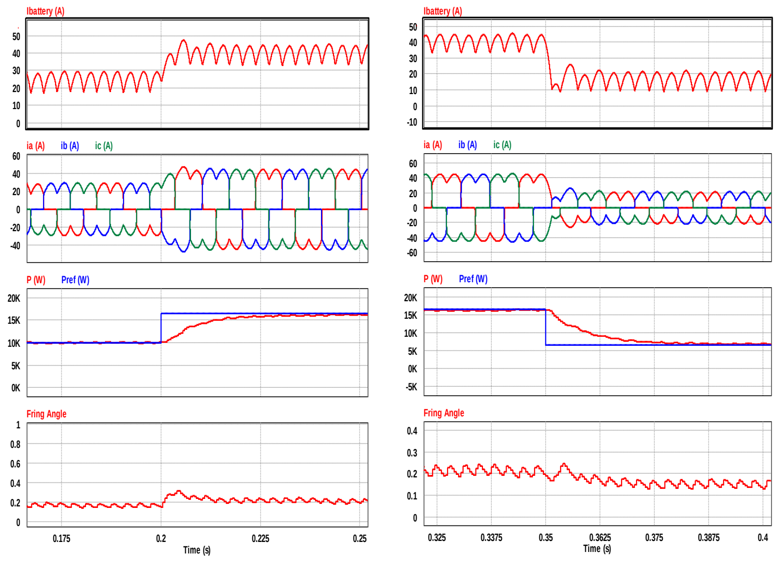

Figure 6 The zoomed battery voltage, battery current, three phase currents, active power and SCR firing angle obtained from proposed controller (a)The transition from 10kW to 16kW,(b)The transition from 16kW to 6kW

The experimental prototype of the proposed controller for the battery chargers is shown in Figure 7. The experimental system includes voltage sensors, current sensors, inductors, the chargers power module, DSP board. The battery voltage, battery current, three-phase line voltages V_a , V_b and V_c are measured by the voltage and current sensors.

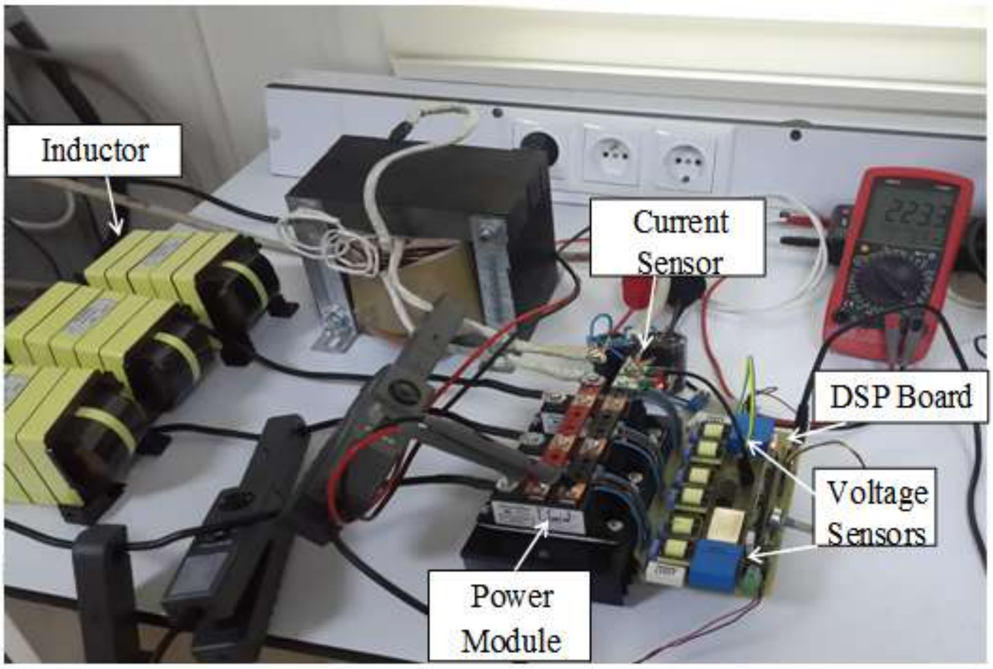

Figure 7 Experimental prototype of DSP based proposed controller for battery chargers

The SCR is used for the semiconductor switch in chargers power module. A TI -F28335 DSP is used for application of control algorithm. The DSP has a 32-bit floating point, two groups of 16-bit three-phase PWM outputs, different serial port peripherals, two 32-bit quadrature encoder interfaces and 16 ADC module.

Figure 8 shows the battery voltage and current values obtained from digital phosphor oscilloscope during the charging process for the proposed controller of the battery chargers. As shown in Figure 8, the battery voltage first increases while the battery current is constant about 9.5A. The battery current decreases while the battery voltage is constant about 250V.

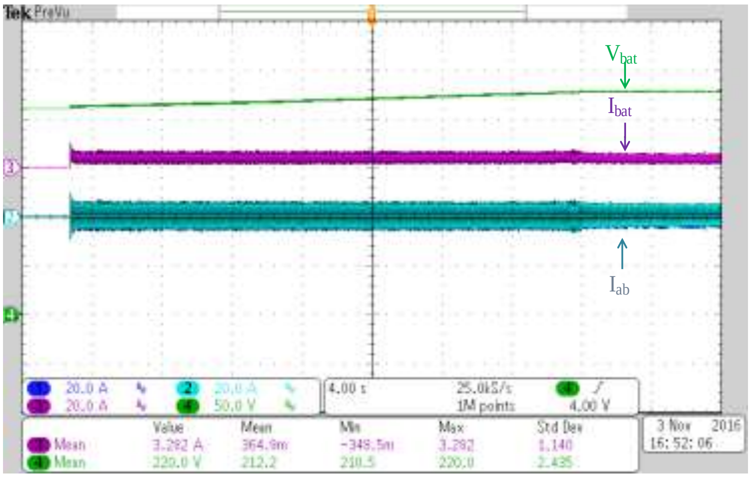

Figure 8 Battery voltage and current values obtained from digital phosphor oscilloscope during the charging process

Figure 9 shows the system transient response to a disturbance on the phase current. The system transient response to the phase current that is stepped up from 33.33% to 100% is shown. The system transient response to the phase current that is stepped down from 100% to 33.33% is shown. The proposed controller of the battery charger responds to the current commands rapidly.

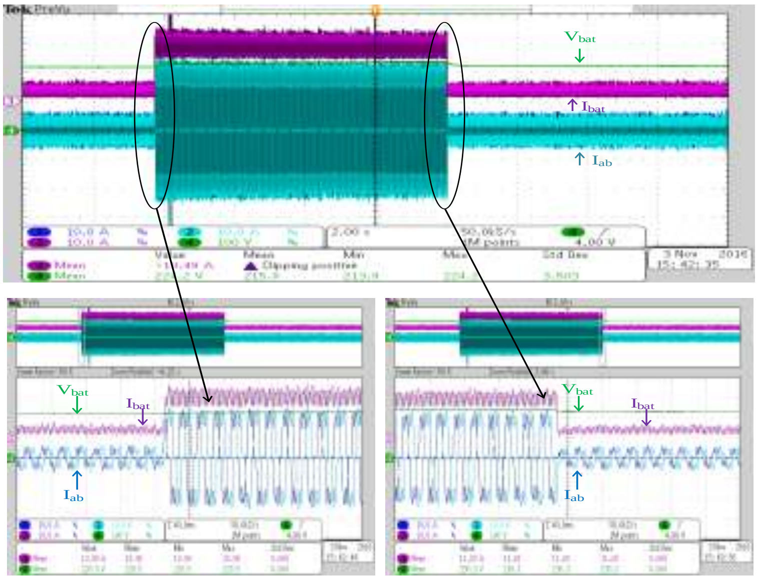

Figure 9 The transient response to a disturbance on the phase current, the transition from charging operation, the phase current from 33.33% to 100 % with zoomed version and the phase current from 100% to 33.33% with zoomed version

The performance of the proposed controller of the battery chargers is tested for the battery voltage and current commands. The experimental results of the proposed controller are shown in Figure 10.

Figure 10a shows the system charging operation on the battery voltage and current. The battery voltage began from 200V and it arrived 250V. The battery current began from 9.5A, and it arrived 0A. Variable battery voltage and stable battery current are shown in Figure 10b. Stable battery voltage and variable battery current are shown in Figure 10c. As the battery voltage increases, the battery current stays at the constant value and then, as the battery voltage stays at the constant value, the battery current decreases.

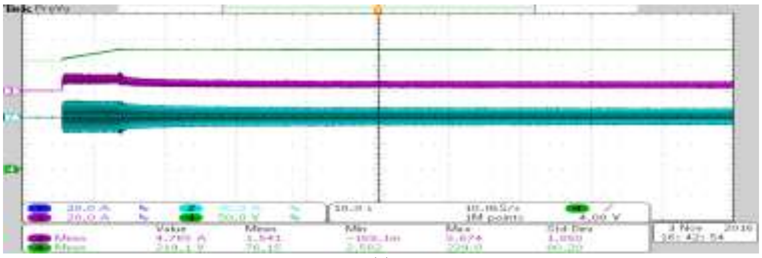

(a)

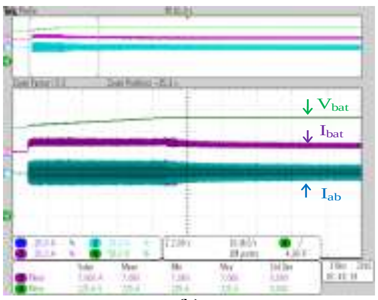

(b)

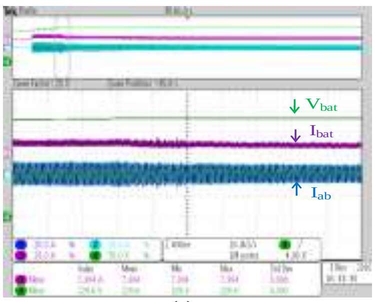

(c)

Figure 10 The experimental results of the proposed controller (a)The system charging operation on the battery voltage and current, (b)Variable battery voltage and stable battery current with zoom factor 5X (c)Stable battery voltage and variable battery current with zoom factor 25X

IV. CONCLUSIONS

The DSP based new controller using embedded code generation ECG for the battery charger has been designed, simulated and implemented in the laboratory. Battery charger consists of a three-phase SCR rectifier which is suitable for high power outputs such as induction heating and DC arc furnaces. The proposed controller is developed by using of computational PLL and C blocks in PSIM. The proposed controller is transmitted to SimCoder to obtain C-code. SimCoder generates all project outputs to the CCS. The CCS loads the generated code to the DSP. In a battery charge controller design, when the users request to modify the codes for DSP and create a prototype, as well as creating C codes for CCS; the embedded code generation ECG provides a very fast solution. The proposed controller adjusts the battery voltage and the battery current. The battery voltage first increases while the battery current is constant about 9.5A. The battery current decreases while the battery voltage is constant about 250V. Experimental and simulation studies show that the proposed controller for the battery chargers has a rapid dynamic response, good steady state performance, they are quite simple, understandable and easy to implement.

REFERENCES

[1]. Chuang, Y. C.: High-efficiency ZCS buck converter for rechargeable batteries. IEEE T Ind. Electron. 57, 2463–2472 (2010)
[2]. Khaligh, A., Li, Z.: Battery, ultra capacitor, fuel cell, and hybrid energy storage systems for electric, hybrid electric, fuel cell, and plug-in hybrid electric vehicles: State of the art. IEEE T Vehicle. Technol. 59, 2806–2814 (2010).
[3]. Hamza, D. Pahlevaninezhad, M. Jain, P.: Implementation of a novel digital active EMI technique in a DSP-based DC-DC digital controller used in electric vehicle (EV) Battery charger. IEEE T Power Electronics 99: 1-10 (2013)
[4]. Yilmaz, M. Krein, P. T.: Review of battery charger topologies, charging power levels, and infrastructure for plug-In electric and hybrid vehicles. IEEE T Power Electronics. 28, 2151-2169 (2013)
[5]. Wang, C. S., Stielau, O. H., Covic, G. A.: Design considerations for a contactless electric vehicle battery charger. IEEE Trans. Ind. Electron. 52, 1308-1314 (2005)
[6]. Tremblay, O., Dessaint, L. A., Dekkiche, A. I.: A generic battery model for the dynamic simulation of hybrid electric vehicles. Proc. IEEE Veh. Power Propulsion Conf. 284-289 (2007)
[7]. Sallan, J., Villa. J. L., Liombart. A. J., Sanz, F.: Optimal design of ICPT systems applied to electric vehicle battery charge. IEEE Trans. Ind. Electron. 56, 2140-2149 (2009)
[8]. Sripakagorna, A., Limwuthigraijirat, N.: Experimental assessment of fuel cell/supercapacitor hybrid system for scooters. Int J Hydrogen. Energy. 34, 6036-6044 (2009)
[9]. Arce, A., del Real, A. J., Bordons, C.: MPC for battery/fuel cell hybrid vehicles including fuel cell dynamics and battery performance improvement. J Process Control. 19, 1289-1304 (2009)
[10]. Chuang, Y. C., Ke ,Y. L.: A novel high-efficiency battery charger with a buck zero-voltage-switching resonant converter. IEEE T. Energy Conver. 22, 848–854 (2007)
[11]. Kemadish, A., Kaabi, A. L., Fardoun, A. A., Ismail, E. H.: Bridgeless high voltage battery charger PFC rectifier. Renew. Energy 56, 24-31 (2013)
[12]. Hu, Y., Song, X., Cao, W., Ji, B.: New SR drive with integrated charging capacity for plug-in hybrid electric vehicles (PHEVs). IEEE Trans. Ind. Electron. 61, 5722-5731 (2014)
[13]. Gu, B., Lin, C., Chen, B., Dominic, J., Lai, J.: Zero-voltage-switching PWM resonant full-bridge converter with minimized circulating losses and minimal voltage stresses of bridge rectifiers for electric vehicle battery chargers. IEEE T. Power Electronics. 28, 4657–4667 (2013)
[14]. Ladoux, P., Postiglione, G., Foch, H., Nuns, J.: A comparative study of ac/dc converters for high-power dc arc furnace. IEEE T Ind. Electron. 52, 747–757 (2005)
[15]. Srdic, S., Nedeljkovic, M.: Predictive fast DSP-based current controller for thyristor converters. IEEE T Ind. Electron. 58, 3349-3358 (2011)
[16]. Rodriguez, J. R., Pontt, J., Silva, C., Wiechmann, E. P., Hammond, P. W., Santucci, F. W., Alvarez, R., Musalem, R., Kouro, S., Lezana, P.: Large current rectifiers: State of the art and future trends. IEEE T Ind. Electron. 52, 738–746 (2005)
[17]. Chen, B. Y., Lai, Y. S.: New digital-controlled technique for battery charger with constant current and voltage control without current feedback. IEEE Trans. Ind. Electron. 59, 1545-1553 (2012)
[18]. Masoum, M. A. S., Badejani, S. M., Fuchs, E. F. Microprocessor- controlled new class of optimal battery chargers for photovoltaic applications. IEEE T Energy Conver. 19: 599-606 (2004)
[19]. Muoka, P. I., Haque, M. E., Gargoom, A. A.: Digital signal processor controlled smart battery charger for photovoltaic power systems. Aust. J. Electrical and Electronics Eng 11, 400-410 (2014)
[20]. Hong, K. H., Gan, W. S., Chong, Y. K., Chew, K. K., Lee, C. M., Koh, T. Y.: An integrated environment for rapid prototyping of DSP algorithms using Matlab and Texas Instruments, TMS320C30. Microprocess Microsy. 24, 349–363 (2000)
[21]. Kesler, M., Kisacikoglu, M. C., Tolbert, L. M.: Vehicle-to-grid reactive power operation using plug in electric vehicle bidirectional off board charger. IEEE T Ind Electron. 61, 6778-6784 (2014)

Yasemin ÖNAL†" DSP Based Battery Charger Control System Using Embedded Code Generation for Thyristor Rectifier" American Journal of Engineering Research (AJER), vol.8, no.07, 2019, pp.116-123